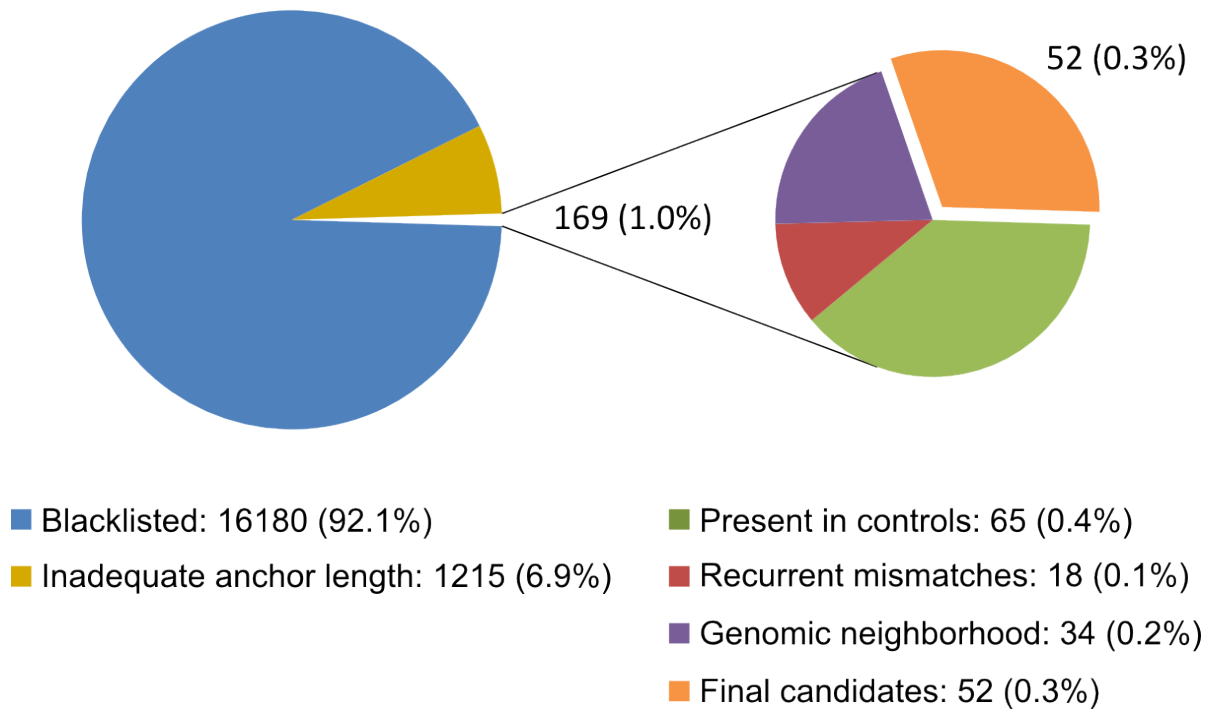


Supplementary Figure 1 | Schematic of the process used for fusion discovery and for filtering fusion candidates.

145 848 total reads aligned to fusion junctions.
Total of 17 564 fusion candidates.



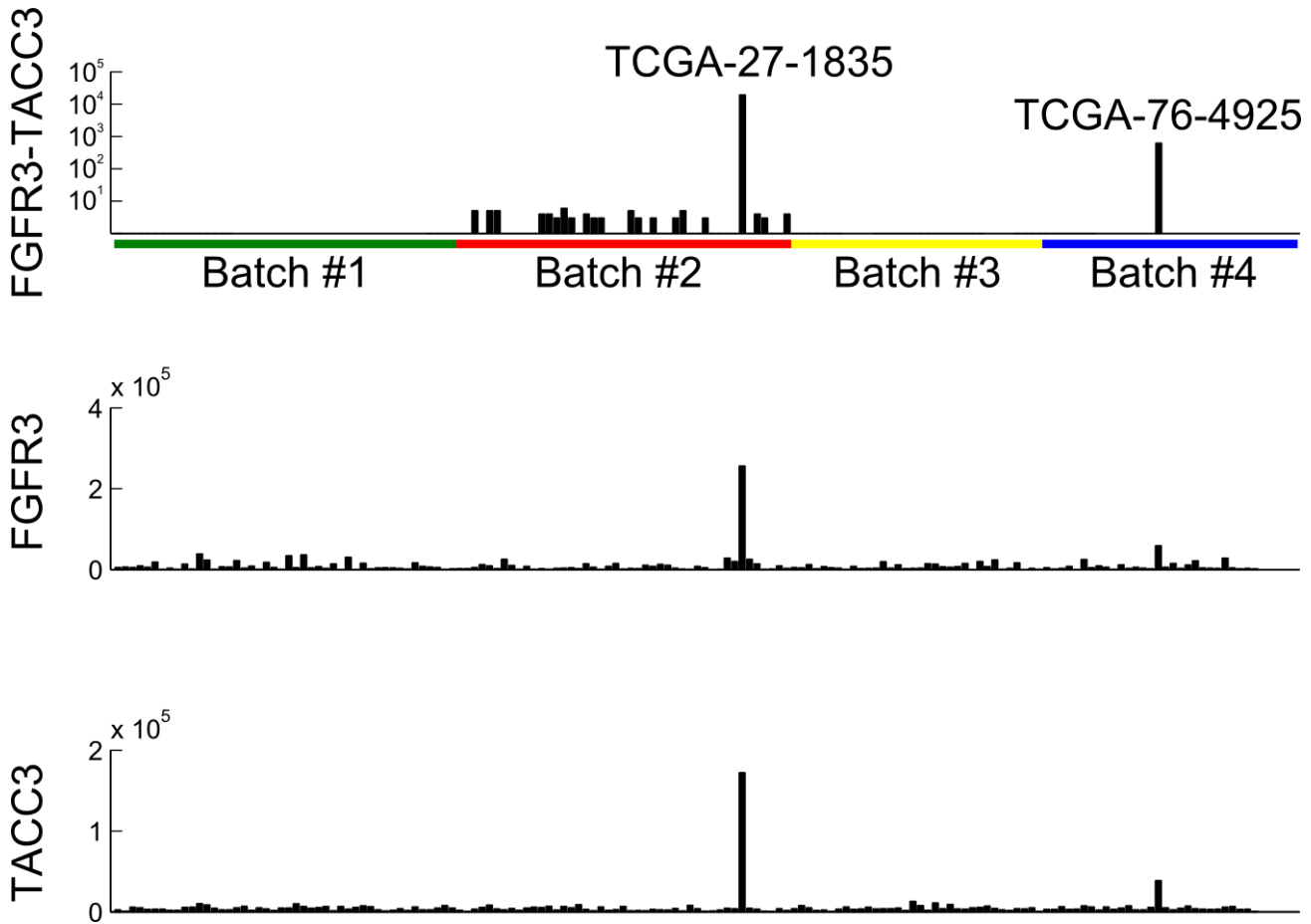
Supplementary Figure 2 | Total number of discovered fusion candidates in all 10 sample pools and after consecutive filtering based on different criteria. The filters were applied in the following order: blacklisted genes, inadequate anchors, presence in negative controls, recurrent mismatches in alignments.

FGFR3 exon 18

TACC3 exon 11

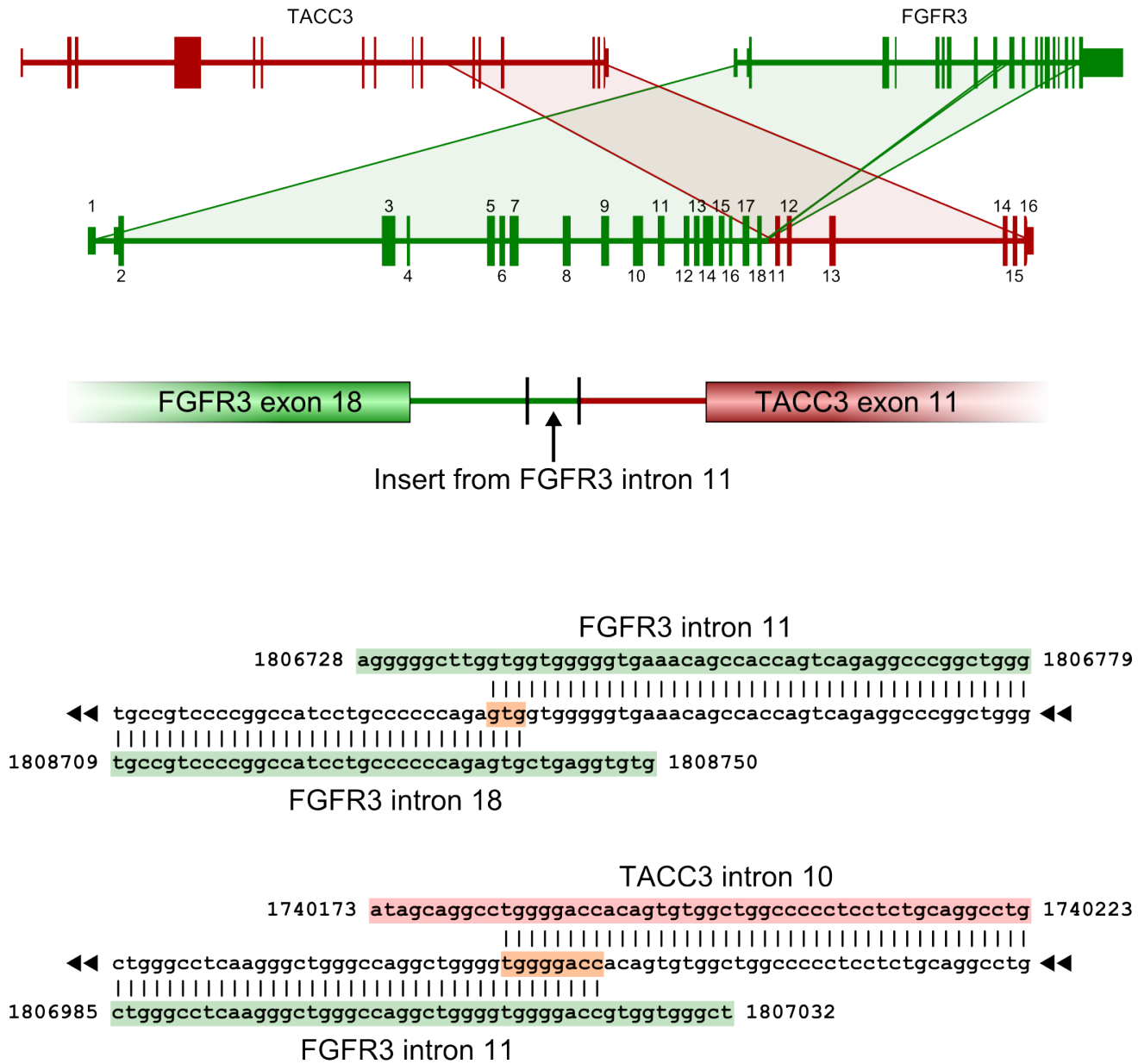
GGACCTGGACCGTGTCCTTACCGTGACGTCCACCGAC	GTAAAGGCGACACAGGAGGAGAACCGGGA
GGACCTGGACCGTGTCCTTACCGTGACGTCCACCGAC	GTAAAGGCGAC
GGACCTGGACCGTGTCCTTACCGTGACGTCCACCGAC	GTAAAGGCGAC
GGACCTGGACCGTGTCCTTACCGTGACGTCCACCGAC	GTAAAGGCGAC
GGACCTGGACCGTGTCCTTACCGTGACGTCCACCGAC	GTAAAGGCGAC
GGACCTGGACCGTGTCCTTACCGTGACGTCCACCGAC	GTAAAGGCGAC
GGACCTGGACCGTGTCCTTACCGTGACGTCCACCGAC	GTAAAGGCGAC
GGACCTGGACCGTGTCCTTACCGTGACGTCCACCGAC	GTAAAGGCGAC
GGACCTGGACCGTGTCCTTACCGTGACGTCCACCGAC	GTAAAGGCGAC
GGACCTGGACCGTGTCCTTACCGTGACGTCCACCGAC	GTAAAGGCGAC
GGACCTGGACCGTGTCCTTACCGTGACGTCCACCGAC	GTAAAGGCGAC
GGACCTGGACCGTGTCCTTACCGTGACGTCCACCGAC	GTAAAGGCGAC
GGACCTGGACCGTGTCCTTACCGTGACGTCCACCGAC	GTAAAGGCGAC
CTGGACCGTGTCCTTACCGTGACGTCCACCGAC	GTAAAGGCGACACAG
CCGTGTCCTTACCGTGACGTCCACCGAC	GTAAAGGCGACACAGGAGGA
CCGTGTCCTTACCGTGACGTCCACCGAC	GTAAAGGCGACACAGGAGGA
CCGTGTCCTTACCGTGACGTCCACCGAC	GTAAAGGCGACACAGGAGGA
TACCGTGACGTCCACCGAC	GTAAAGGCGACACAGGAGGAGAACCGGGA

Supplementary Figure 3 | RNA-seq reads indicate a fusion between *FGFR3* exon 18 and *TACC3* exon 11 in a GBM sequencing pool that included patient GBM-13. The genomic reference is indicated in bold.



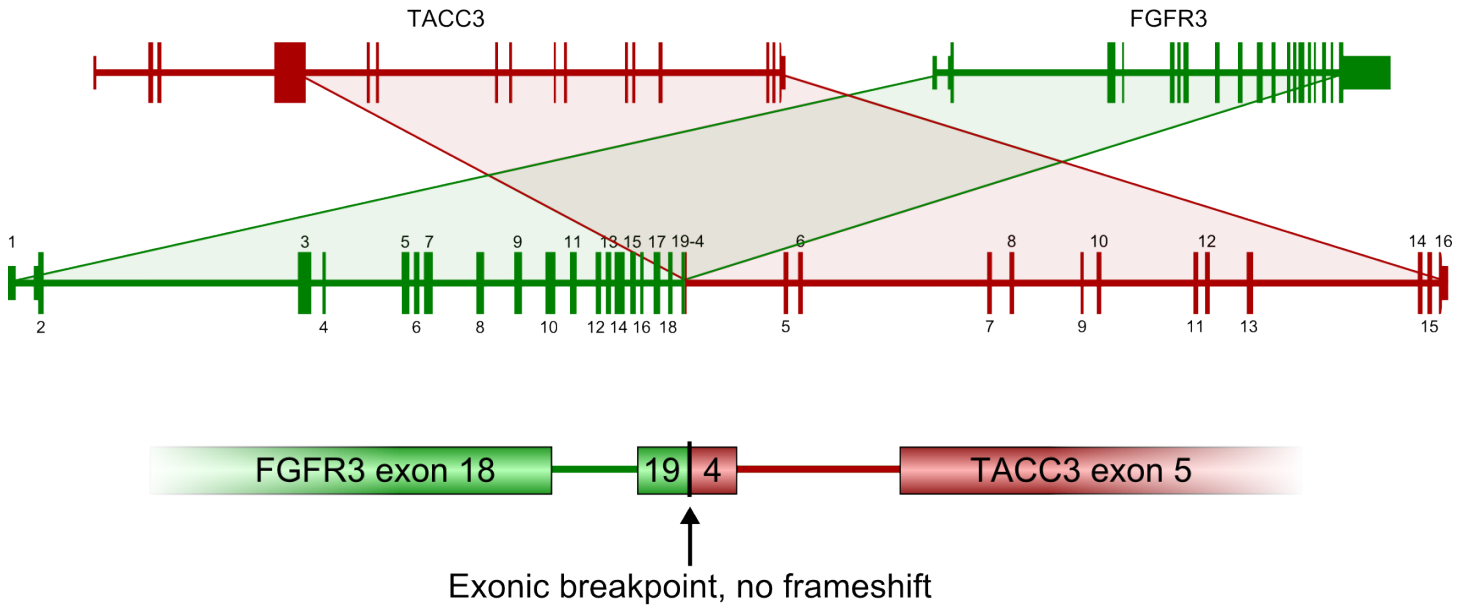
Supplementary Figure 4 | Transcriptome sequencing data from the Cancer Genome Atlas GBM project reveals two fusion positive tumors. We also observed that other samples in the same batch as the strongly fusion expressing sample TCGA-27-1835 have been contaminated with *FGFR3-TACC3* transcripts.

GBM-13 DNA sequencing



Supplementary Figure 5 | DNA-level schematic of *FGFR3-TACC3* in patient GBM-13 based on genomic DNA PCR and Sanger sequencing. A short fragment of *FGFR3* intron 11 is inserted at the breakpoint between *FGFR3* and *TACC3*. The shared nucleotide sequences are shown in peach.

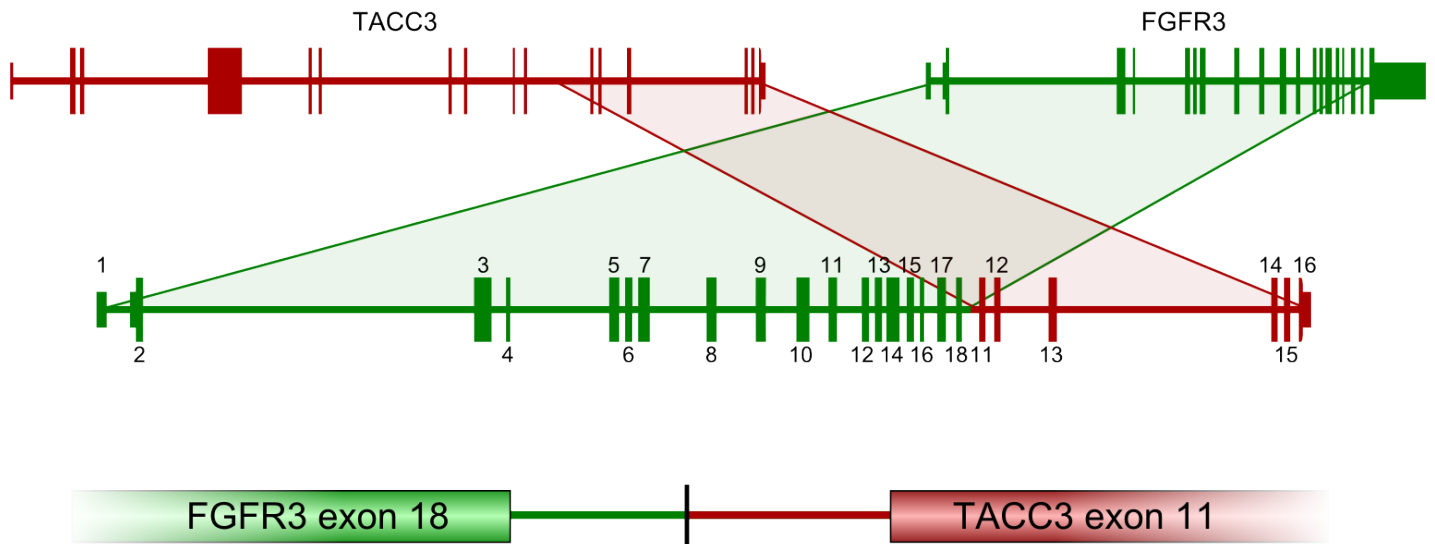
GBM-07 DNA sequencing



TACC3 exon 4
 1730499 gtcctgtctgagccagtaagtgtgaggatgggatggggagcgtg 1730543
 |||
 ◀◀ cctggacctgtcggcgcctttcgagcagtactccccgagccagtaagtgtgaggatgggatggggagcgtg ◀◀
 |||
 1808848 cctggacctgtcggcgcctttcgagcagtactccccgggtggccagg 1808894
 FGFR3 exon 19

Supplementary Figure 6 | DNA-level schematic of *FGFR3-TACC3* in patient GBM-07 based on genomic DNA PCR and Sanger sequencing. The breakpoint interrupted exon 19 of *FGFR3* and exon 4 of *TACC3*, forming a chimeric exon. No frameshift was produced. The shared nucleotide is shown in peach.

GBM-T01 DNA sequencing



TACC3 intron 10

1740552 ttgacgggaaggacggttaggaacaggtaactcaagggtgacttaggtcagagc 1740604

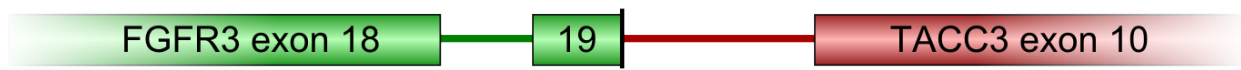
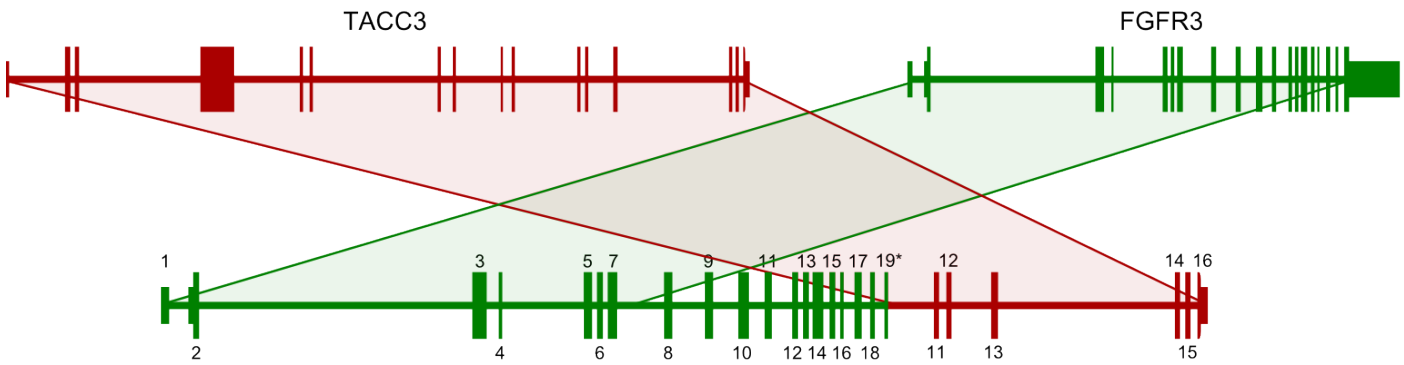
◀◀ cgctatgccctccccctgcccggccggttaggaacaggtaactcaagggtgacttaggtcagagc ▶▶

1808691 cgctatgccctccccctgcccggccatcctcccc 1808732

FGFR3 intron 18

Supplementary Figure 7 | DNA-level schematic of *FGFR3-TACC3* in patient GBM-T01 based on genomic DNA PCR and Sanger sequencing. The shared nucleotide sequence is shown in peach.

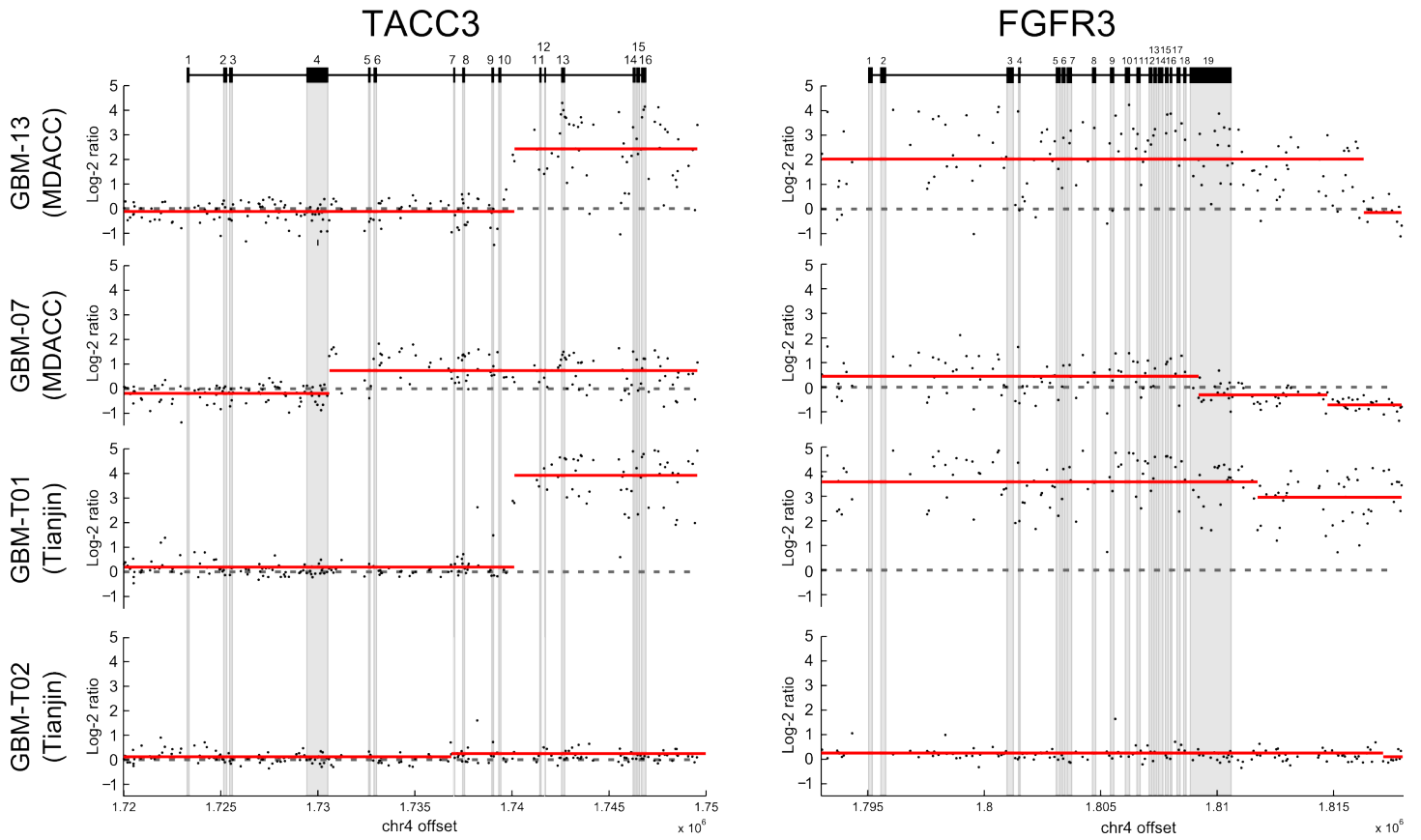
GBM-T02 DNA sequencing



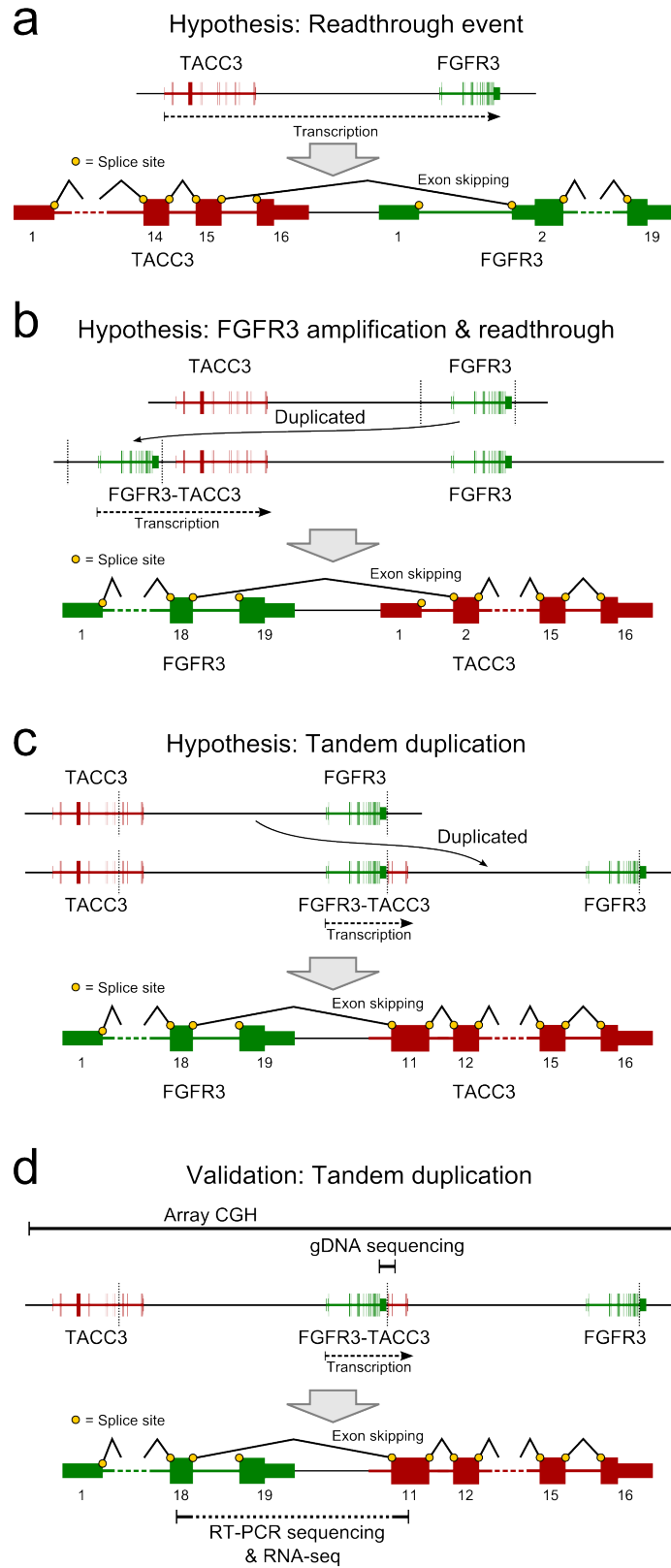
Exonic breakpoint, no frameshift



Supplementary Figure 8 | DNA-level schematic of *FGFR3-TACC3* in patient GBM-T02 based on genomic DNA PCR and Sanger sequencing. The shared nucleotide sequence is shown in peach.

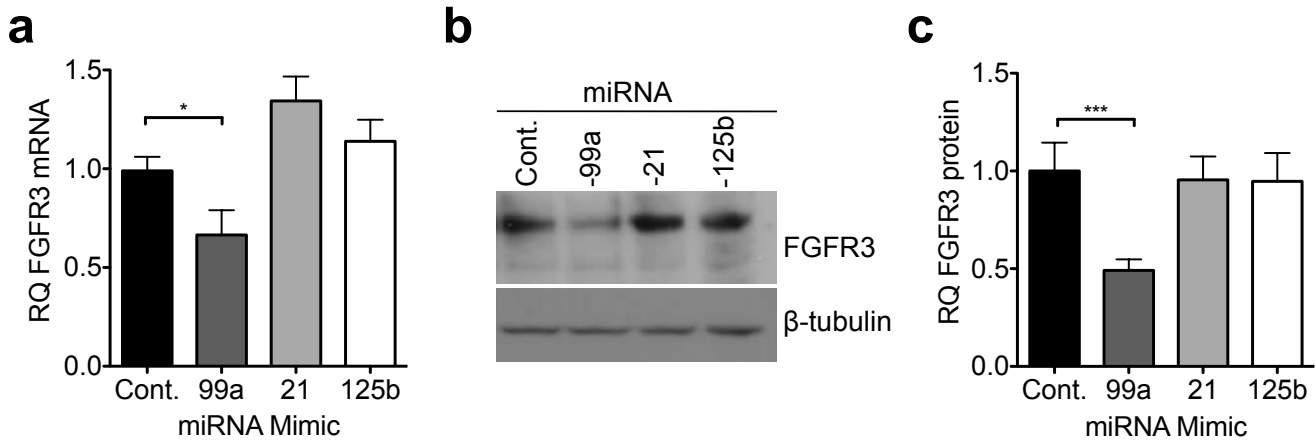


Supplementary Figure 9 | Detailed view of segmented probe logratios for the three fusion positive patients on the Agilent custom aCGH chip. Gene exon structures are shown at the top in black. In patients GBM-13 and GBM-T01, the TACC3 breakpoint was situated between exons 10 and 11; in GBM-07 it interrupted exon 4; in GBM-T02 it was between exons 9 and 10. There was considerable variation in the *FGFR3* breakpoint locations across samples.

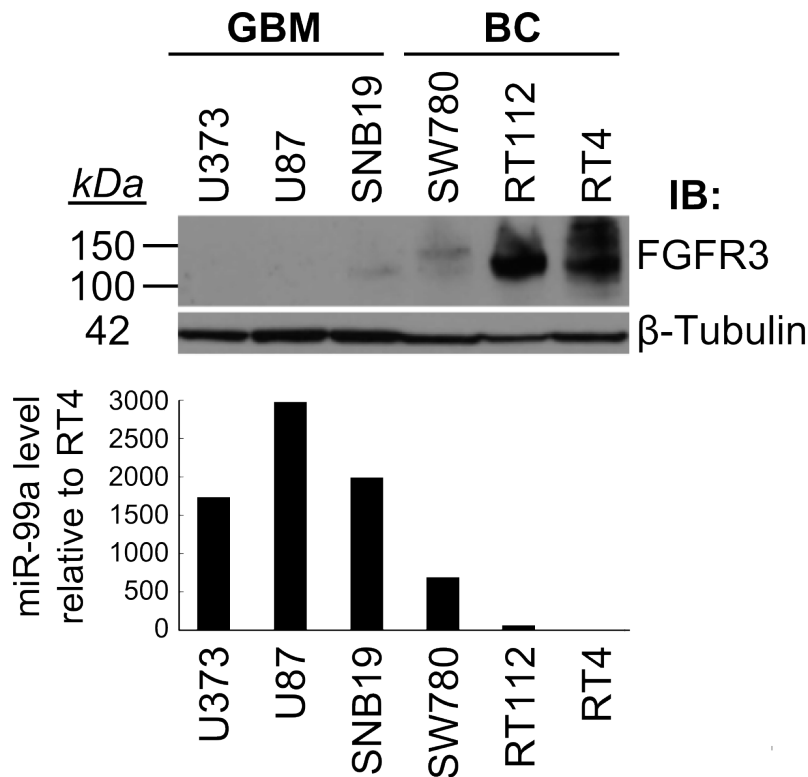


Supplementary Figure 10 | Alternative hypotheses for the mechanism generating the *FGFR3-TACC3* fusion. a) A read-through event is ruled out by *TACC3* being upstream of *FGFR3*. b) *FGFR3* amplification and translocation upstream of *TACC3* is ruled out by the fact that observed fusions only

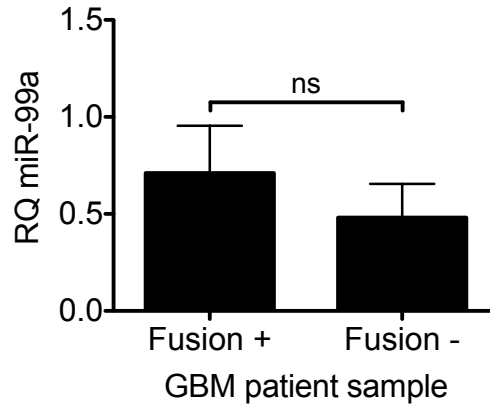
involve *TACC3* exons 5 and forward, and by the aCGH data which indicates a larger amplicon involving parts of *TACC3*. c) A tandem duplication can explain the observed fusion genes. d) Different experiments through which the presence of the tandem duplication was validated.



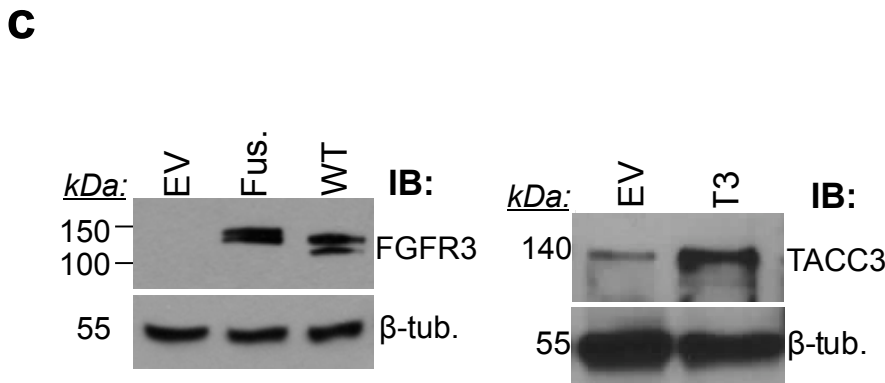
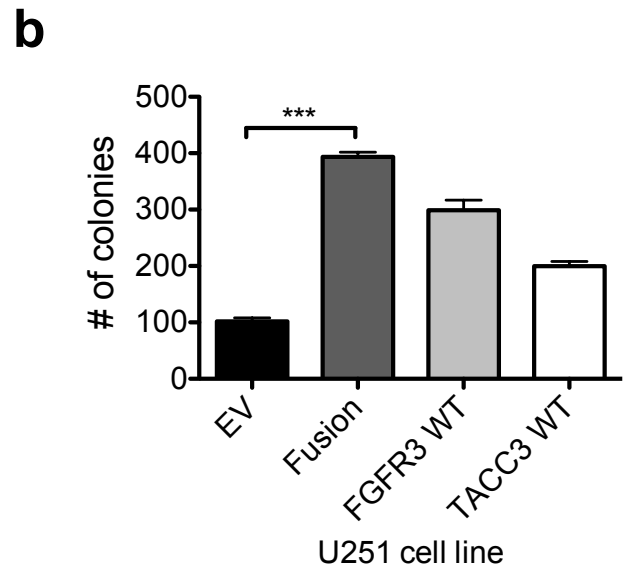
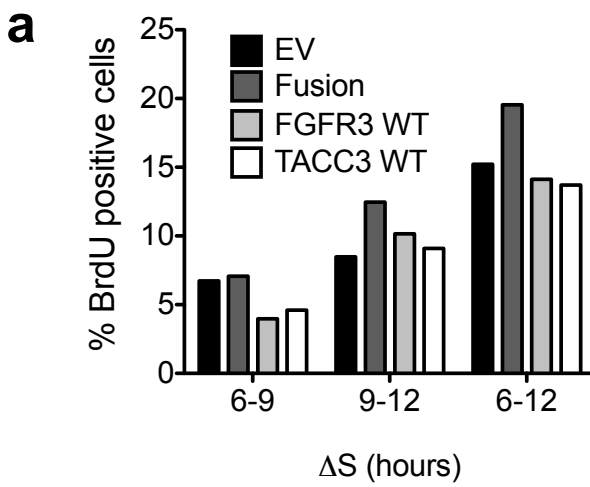
Supplementary Figure 11 | Of the highest expressed miRNA in GBM, only miR-99a suppresses *FGFR3* expression. Upon miR-99a, -21, or -125b transfection, relative *FGFR3* mRNA or protein levels were measured by qRT-PCR (a), immunoblotting (b), and densitometry (c), respectively. Error bars, s.e.m.; P-values calculated using Student's t-test. *P<0.05; *P<0.001.**



Supplementary Figure 12 | *FGFR3* immunoblot and miR-99a qRT-PCR for 3 glioblastoma and 3 bladder cancer (BC) cell lines. *FGFR3* protein level is inversely correlated with miR-99a.

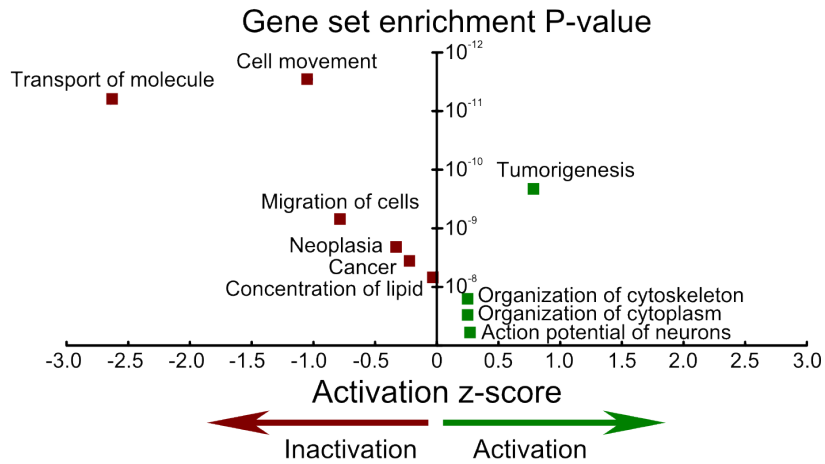


Supplementary Figure 13 | Relative levels of miR-99a were tested via qRT-PCR between fusion positive (n=4) and negative (n=8) patient samples. No significant difference between groups was observed (p = 0.46; two-tailed Student's t-test), suggesting the fusion does not regulate miR-99a expression. Relative miR-99a expression was normalized to endogenous U6 expression. Error bars, median absolute deviation.

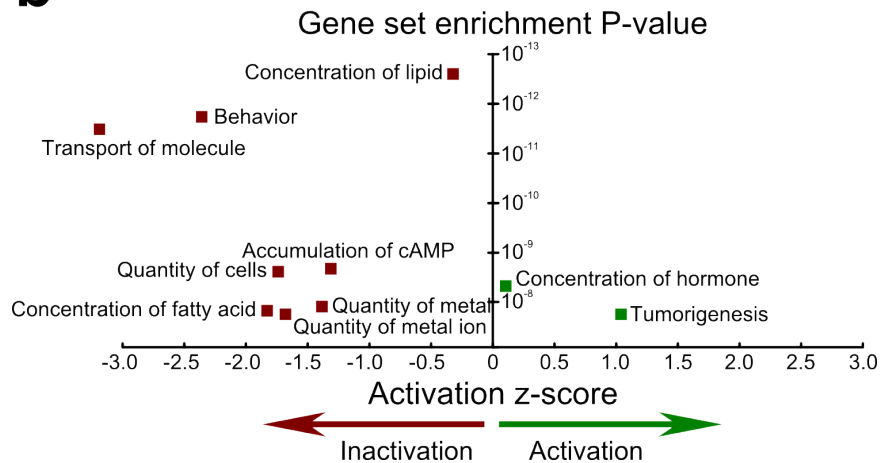


Supplementary Figure 14 | U251 cell line behaves similar to SNB19 when engineered to overexpress EV, fusion, wt *FGFR3*, or wt *TACC3* constructs. BrdU analysis (a) and soft-agar colony formation studies were performed on U251 stable cell lines. U251 fusion expressing cells grew significantly more colonies in soft agar (p=0.0001). Also, wt *FGFR3* cells also grew significantly more colonies (p= 0.0005). (d). Immunoblot of U251 stable cell lines, expressing EV, Fusion (Fus.), wt *FGFR3* (WT), or wt *TACC3* (T3) constructs (f). Error bars, s.e.m.; P-values calculated using two-tailed student's t-test. ***P<0.0001.

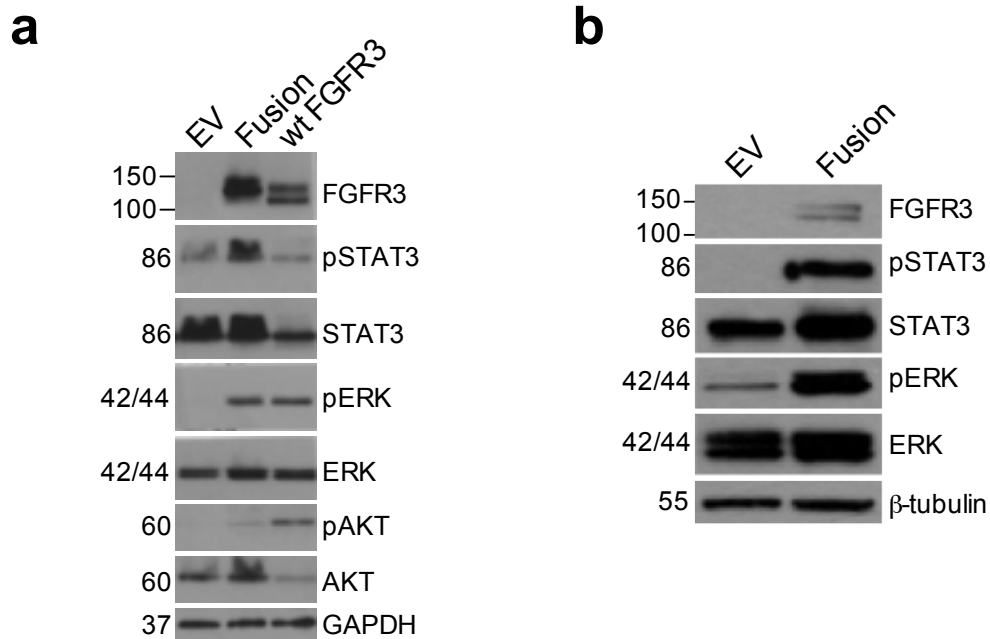
a



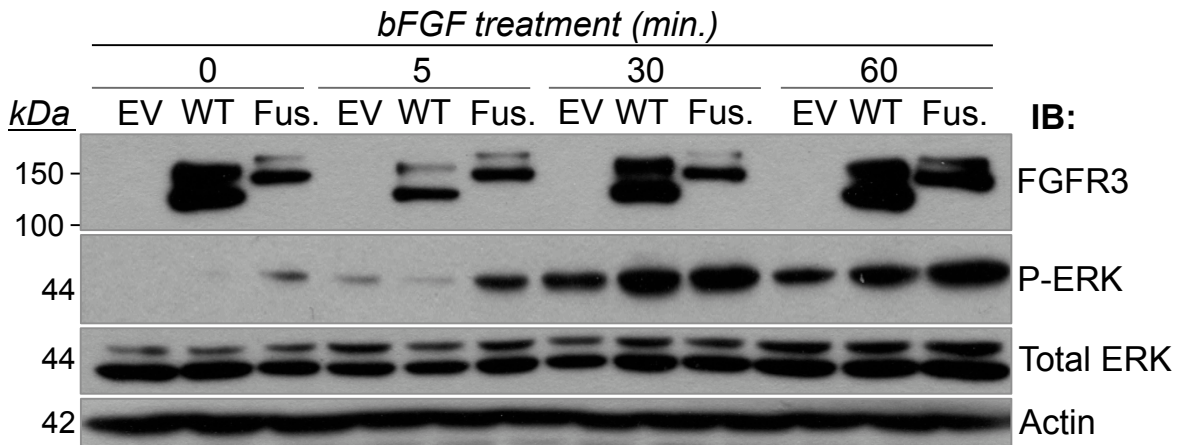
b



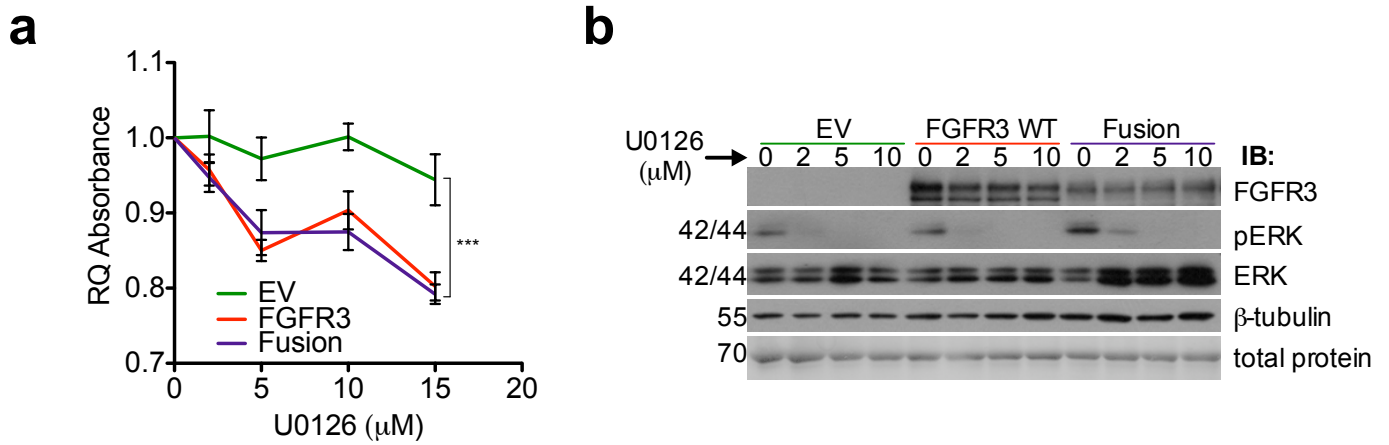
Supplementary Figure 15 | Top ten altered pathways identified by Ingenuity Pathway Analysis (IPA) for differential gene expression between SNB19 cell lines transfected with wt *FGFR3* and those transfected with empty vector (a), or wt *TACC3* and empty vector (b). Positive regulation z-scores indicate increased pathway activation. Only the top nine pathways are shown because IPA analysis did not allocate a regulation z-score for the next gene sets.



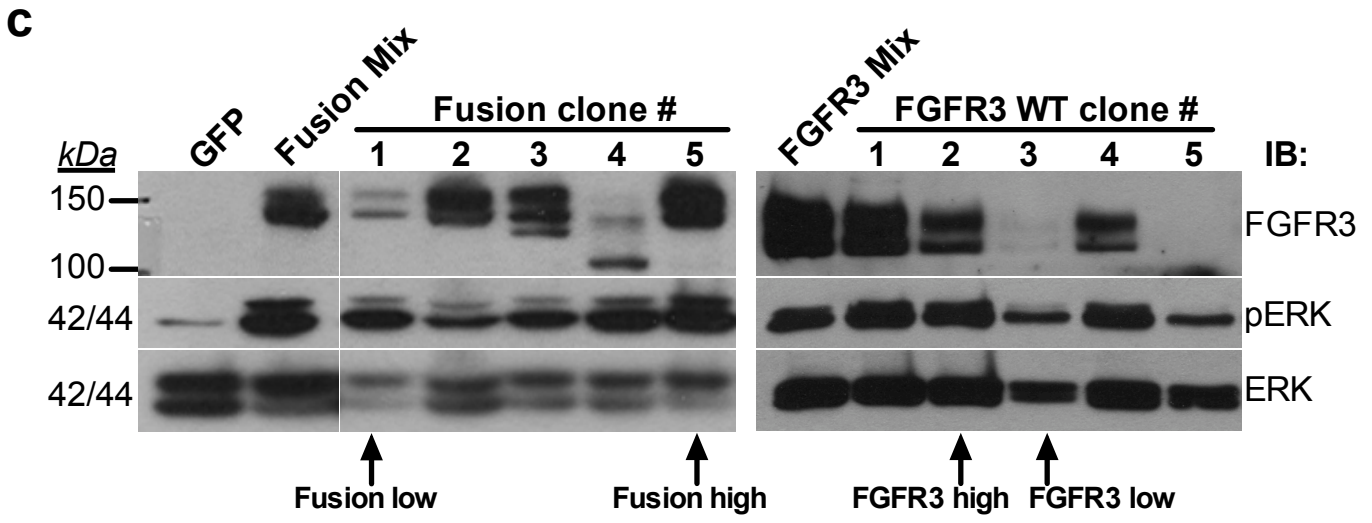
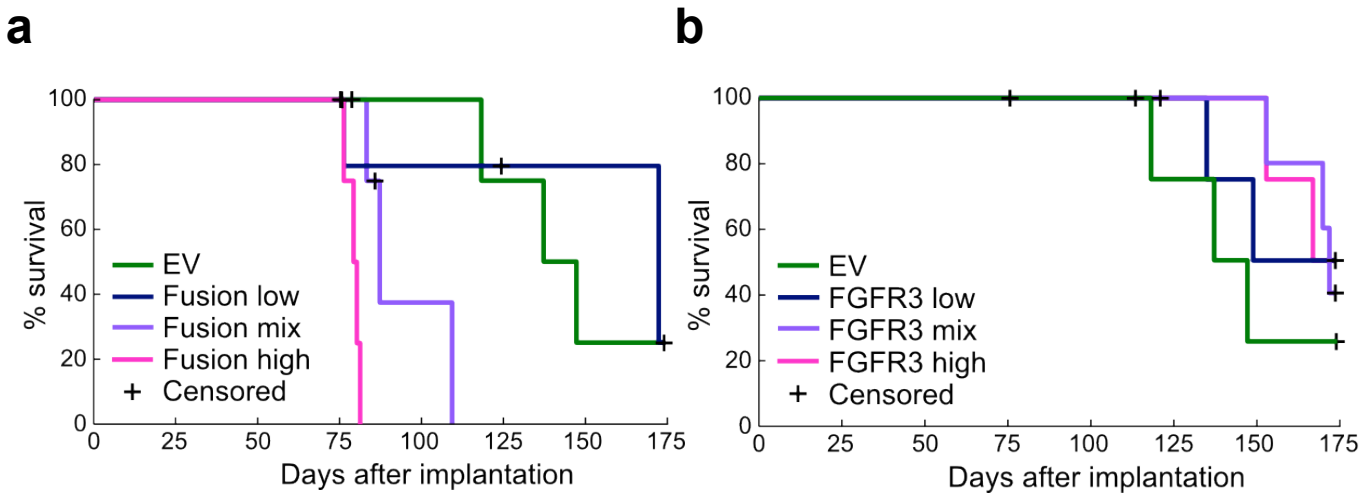
Supplementary Figure 16 | Downstream analysis of transient (a) and stable (b) fusion cell lines indicate the major downstream molecules activated are STAT3 and ERK. AKT is not significantly activated by the presence of the fusion.



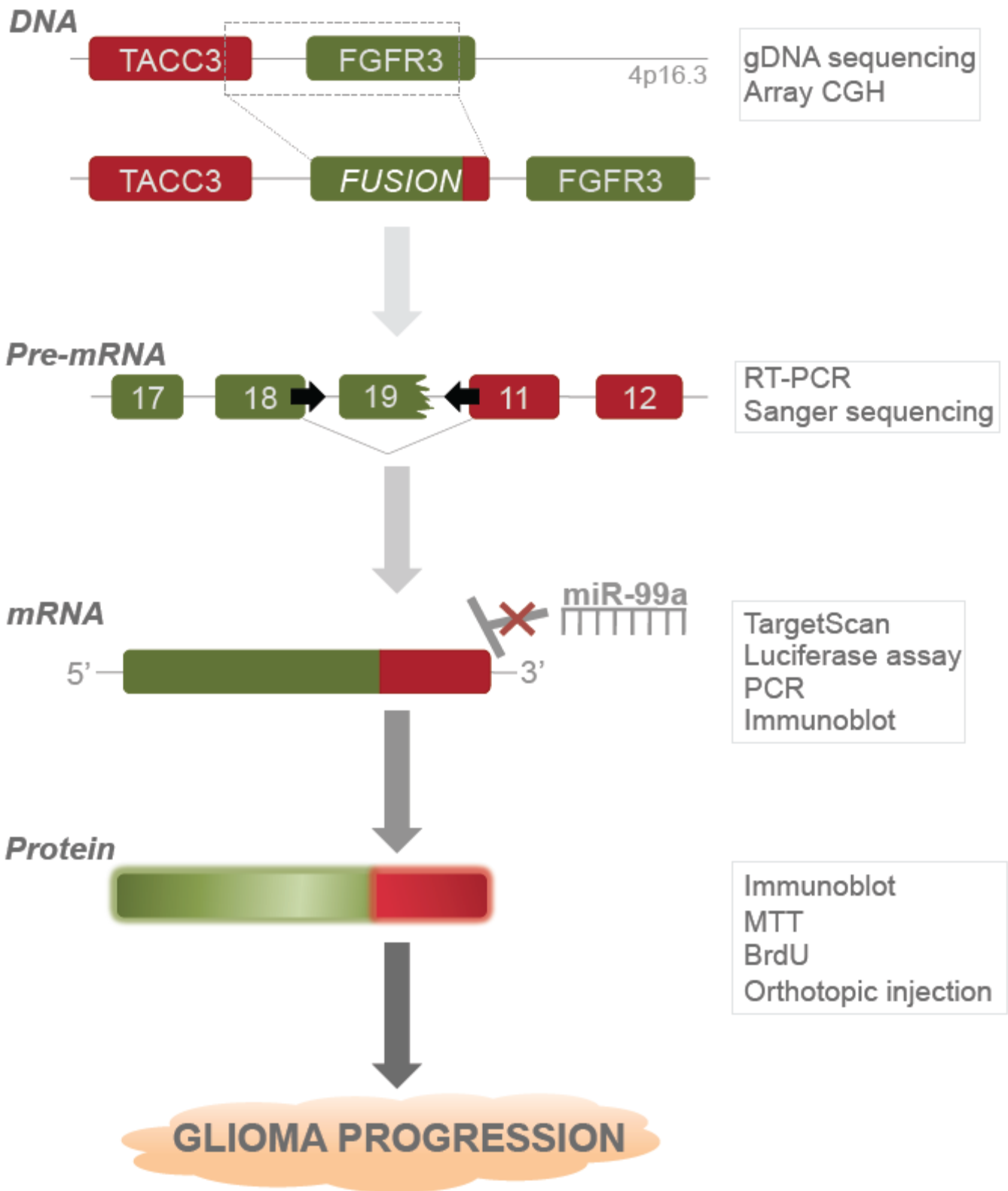
Supplementary Figure 17 | EV, wt *FGFR3* (WT) or Fusion (Fus.) overexpressing cell lines were serum starved and then incubated with bFGF ligand for the indicated times. All cell lines exhibited ligand-dependent ERK activation, although the fusion did show a slight increase in ERK activation in serum starved conditions. However, peak ERK activation was achieved upon incubation with ligand.



Supplementary Figure 18 | Cell viability assay of fusion, wt *FGFR3*, or EV cells treated with increasing concentration of ERK inhibitor U0126 (a). Immunoblot illustrating potency of U0126 (b)



Supplementary Figure 19 | Survival curves of fusion (a) or wt *FGFR3* (b) orthotopically implanted cell lines. SNB19 cell lines were transfected with either fusion or WT cDNA constructs and stable clones selected. Subsequent protein expression is can be visualized via immunoblot (c).



Supplementary Figure 20 | Schematic of the entire process of fusion discovery and further validation.

mRNA sequence for fusion variant 1 (NM_000142.4 bases 1-2530 + NM_006342.2 bases 2097-2837):

```
gtgcgggcagctggcgccgcccggctctgctctgcccgttcgacggagcgcacgggcccggccggccggagggagcggggcgggagctgggcccggcggg  
cagcggagccggagcgggagccgcccgttagcggagccgggctcccggcgtcggcaagtctcccggagcggcccccggctcccggcggctgcccggcggcggcggcgt  
ggggggcagcatgcccgccgcccgtgctgaggacgcgcgggcccggcggcggcggcA TGGGGGCCCTGCCTGCGCCCTCGCGCTCTCGCTGGCCGTGGC  
CATCGTGGCCGGCCTCTCGGAGTCCCTGGGGACGGAGCAGCGCGTCTGGGGCGGAGCGGCAGAAGTCCCggggccCAGAGCCGGCCAGCAGGAGCAG  
TTGGTCTTCGGCAGCGGGGATGCTGTGGAGCTGAGCTGTCCCCGGCCGGGGGTGGTCCCATGGGGCCACTGTCTGGGTCAAGGATGGCACAGGGCTGG  
TGCCCTCGGAGCGTGCCTGGTGGGGCCCCAGCGGCTGCAGGTGCTGAATGCC TCCCACGAGGACTCCGGGGCCTACAGCTGCCGGCAGCGGCTCACGCA  
GCGCGTACTGTGCCACTTCAAGTGTGCGGGTGCAGACGCTCCATCCTCGGGAGATGACGAAGACGGGGAGGACGAGGCTGAGGACACAGGTGTGGACACA  
GGGGCCCCCTTAC TGGACACGGCCCGAGCGGATGGACAAGAAGCTGCTGGCCGTGCGCGCCGCCAACACCGTCCGCTTCCGCTGCCACGCCCTGGCAACC  
CCACTCCCTCCA TCTCCTGGCTGAAGAACGGCAGGGAGTTCGCGGGCAGCACCGCA TTGGAGGCATCAAGCTGCGGCATCAGCAGTGGAGCTGGTGCAT  
GGAAAGCGTGGTCCCTCGGCGCGGCAACTACACTGCGTCTGTGGAGAACAAAGTTTGGCAGCATCCGGCAGACGTACACCGTGGAGCTGTGGAGCGC  
TCCC CGCACCGGCCCATCCTGCAGCGGGGCTGCCGGCAACCAGACGGCGGTGCTGGGCAGGACGTGGAGTCCACTGCAAGGTGTACAGTGCAGCAC  
AGCCCCACATCCAGTGGCTCAAGCACGTGGAGGTGAATGGCAGCAAGGTGGGCCCGGACGGCACACCCCTACGTTACCGTGTCAAGACGGCGGGCGCTAA  
CACCACCGACAAGGAGCTAGAGGTCTCTCCTTGCACAACGTCACCTTTGAGGACGCGGGGAGTACACCTGCCTGGGGGCAATTCATTGGGTTTTCT  
CATCACTCTGCGTGGCTGGTGGTGTCTGCTGACCGAGGAGGAGCTGGTGGAGGTGACGAGCGGGCAGTGTGTATGCAGGCATCCTCAGCTACGGGGTGG  
GCTTCTTCTGTTTCACTCTGGTGGTGGCGGCTGTGACGCTCTGCCCTGCGCAGCCCCCAAGAAAGGCC TGGGCTCCCCACCGTGCACAAGATCTC  
CCGCTTCCCGCTCAAGGCACAGGTGTCCCTGGAGTCCAACCGCTCCATGAGCTCCAACACACCACTGGTGCAGCATCGCAAGGCTGTCCCTCAGGGGAGGGC  
CCCACGCTGGCCAAATGTCTCCGAGCTCGAGCTGCCTGCCAGCCCCAAATGGGAGCTGTCTCGGGCCGGCTGACCC TGGGCAAGCCCCCTGGGGAGGGC  
GCTTCGGCCAGGTGGTCA TGGCCGAGGCAATCGGCATTGACAAGGACCGGGCCCAAGCTTGCACCGTAGCCGTGAAGATGCTGAAGACAGCATGCCAC  
TGACAAGGACCTGTCGGACCTGGTGTCTGAGA TGGAGATGATGAAGATGATCGGGAACACAAAAACATCATCAACTGCTGGGGCCTGCACGCAGGGC  
GGGCCCTGTACGTGCTGGTGGAGTACGGGCCAAGGTAACCTGCGGGAGTTTCTGCGGGCGCGGGCGCCCCGGGGCTGGACTACTCCTTCGACACCT  
GCAAGCCGCCCGAGGAGCAGCTACCTTCAAGGACCTGGTGTCTGTGCTTACCAGGTGGCCCGGGGCATGGAGTACTTGGCTCCCAGAAGTGCATCCA  
CAGGGACCTGGCTGCCCGCAATGTCTGGTGAACGAGGACAACGCTGATGAAGATCGCAGACTTCGGGCTGGCCCGGGACGTGCACAACCTCGACTACTAC  
AAGAAGACAACCAACGGCCGGCTGCCCGTGAAGTGGATGGCGCCTGAGGCCTGTGTTGACCGAGTCTACACTCACCAGAGTGACGCTGGTCTTTGGGG  
TCCTGCTCTGGGAGATCTTACGCTGGGGGGCTTCCCCTACCCCGGCATCCCTGTGGAGGAGCTCTTCAAGCTGTCTGAAGGAGGGCCACCCGATGGACAA  
GCCCGCAACTGCACACACGACCTGTACATGATCATGCGGGAGTGTGGCATGCCCGCCCTCCCAGAGGCCACCTTCAAGCAGCTGGTGGAGGACCTG  
GACCGTCTCCTTACCGTGACGCTCCACCGACCTAAAGGCGCACACAGGAGAGAACCGGGAGCTGAGGAGCAGGTGTGAGGAGCTCCACGGGAAGAACCTGG  
AACTGGGGAAGATCATGGACAGGTTGGAAGAGGTTGTGTACCAGGCCATGGAGGAAGTTCAGAAGCAGAAGGAAGTTTCCAAGCTGAAATCCAGAAAGT  
TCTAAAAGAAAAAGACCAACTTACCACAGATCTGAAC TCCATGGAGAAGTCTTCTCCGACCTCTTCAAGCGTTTTTGAGAAACAGAAAGAGGTGATCGAG  
GGTACC GCAAGAACGAAGTCACTGAAGAAGTGGTGGAGGATTACCTGGCAAGGATCACCAGGAGGGCCAGAGGTACCAAGCCCTGAAGGCCACG  
CGGAGGAGAAGCTGCAGCTGGCAAACGAGGAGATCGCCAGGTCGGGAGCAAGGCCAGGCGGAAGCGTTGGCCCTCCAGGCCAGCTGAGGAAGGAGCA  
GATGCGCATCCAGTTCGCTGGAGAAGACAGTGGAGCAGAAGACTAAAGAGAACGAGGAGCTGACCAGGATCTGCGACGACCTCATCTCCAAGATGGAGAAG  
ATCTGAcctccacggagccgctgtccccgccccctgtcccgtctgtctgtctgtctgattctcttaggtgtcatgttctttttctgtcttcttct  
aacttttttaaaaactagattgctttgaaaacatgaactcaataaaaagtttcttttcaatttaaacactgaa
```

Amino acid sequence of fusion variant 1:

```
MGAPACALALCVAVAI VAGASSE LGEQRVVGRAAEVFPPEPGQEQQLVFGSGDAVELSCPPPGGGPMGPTVWVKDGTGLVPSERVLVGPQRLQVLNAS  
HEDSGAYSCRQRLTQRLVLFHFSVRVTDAPSSGDEDEDEAEEDTGVDTGAPYWTRPERMDKLLAVPAANTVRFRCPAAGNPTPSISWLKNGREFRGEHR  
IGGIKLRHQQWSLVMSVVPDRGN YTCVVENKFGSIRQTYTLDVLE RSPHRPILQAGLPANQTAVLGS DVEFHCKVYSDAQPHIQWLKHVEVNGSKVGP  
DGTPTYVTVLKTAGANTTDKEVLVLSLHNVT FEDAGEY TCLA GNSIGFSHSAWLVLVPAEELVEADEAGSVYAGILSYGVGFLLFLLVVAVTLCLRLS  
PPKKGLSPTVHKISRFP LKRQV SLESNASMSNTPLVRIARLSSGEGPTLANVSELELPADPKWELSRARLT LGKPLGEGCFQGVVMAEAI GIDKDRAA  
KPVTVAVKMLKDDATDKDLSDLVSEMEMMKMI GKHKNI INLLGACTQGGPLYVLVEYAAKGNLREFLRARRPPGLDY SFDTC KPPPEQLTFKDLVSCAYQ  
VARGMEY LASQKCIHRDLAARNVLVTE DNMVKIADFLGARDVHNLDYKKT TNGRLPVKWMAP EALFDRVYTHQSDVWSFGVLLWEI FTLGGSFPYGP  
EELFKLLKEGHRMDKPANCTH DLYMIMRECWHAAPSQRPTFKQLVEDLDRVLTVTST DVKATQ EENRELRSRCEELHGKNLEL GKIMDRFEVVYQAMEE  
VQKQKELSKAEIQKVLKEK DQLTDLNLSMEKSFSDLFRKFEKQKEVIEGYRKNESLKKVEDYLARITQEGQRYQALKAHAEKQLLANEEIAQVRSKA  
QAEALALQASLRKEQMRIQSLEKTVEQTKENEELTRICDDLISKMEKI-
```


Sample	Fusion variant
MDA GBM-13	FGFR3-TACC3 e18-e11
MDA GBM-07	FGFR3-TACC3 e19*-e4*
Tianjin GBM-T01	FGFR3-TACC3 e18-e11
Tianjin GBM-T02	FGFR3-TACC3 e18-e10
TCGA-27-1835	FGFR3-TACC3 e18-e11
TCGA-12-0826	FGFR3-TACC3 e18-e8
TCGA-06-6390	FGFR3-TACC3 e18-e9
TCGA-19-5958	FGFR3-TACC3 e18-e8
TCGA-76-4925	FGFR3-TACC3 e18-e10
Singh GBM-22	FGFR3-TACC3 e18-e10
Singh GBM-1123	FGFR3-TACC3 e19*-e8
Singh GBM-51	FGFR1-TACC1

Supplementary Table 1 | Summary of all reported *FGFR-TACC* fusions. (*) Breakpoint disrupts an exon.